Vortex Roll-Up from an Elliptic Wing at Moderately Low Reynolds Numbers

Hiroshi Higuchi,* José C. Quadrelli,† and Cesar Farell‡
University of Minnesota, Minneapolis, Minnesota

An experimental investigation of tip-vortex roll-up was undertaken at moderately low Reynolds numbers for an elliptic wing with a NACA 66_2-415 section. Flow visualizations and laser Doppler velocimetry measurements were carried out to examine the flow in the vortex core and the tangential velocity distributions around the core. Separation was observed on both sides of the foil for Reynolds numbers up to 5×10^5. The observed changes in the location of separation and reattachment with angle of attack and Reynolds number were adequately predicted by laminar boundary-layer calculations. Axial and tangential velocity profile measurements were made at Reynolds numbers up to about 5×10^4. The vortex core radius was found to grow with increasing angle of attack, increasing downstream distance, and decreasing Reynolds number. A comparison of the experimentally-determined velocity distributions and core sizes, with the results of inviscid, laminar, and turbulent vortex models, is presented.

Introduction

THE importance of a thorough understanding of the mechanics of tip-vortex roll-up is widely recognized both in the field of aeronautics and in that of naval architecture. The dangers created by tip-vortex wakes of aircraft and the problems associated with propeller cavitation phenomena have prompted a fair number of studies of this problem, including analytical, numerical, and experimental investigations. (See, for example, the reviews of tip-vortex literature by Donaldson and Billanin,[1] Platzer and Souders,[2] and Hoeijmakers,[3] the last one on recent developments in numerical simulations.)

In spite of the various empirical and theoretical models available to date, from the inviscid models of Betz[4] and Prandtl,[5] Moore and Saffman's[6] viscous flow model with axial core flow, and Phillips'[7] turbulent vortex model to Staufenbiel's more recent model,[8] the mechanism of the roll-up process, including, in particular, the growth of the vortex core radius, is yet to be fully understood. Even though model tests in wind and water tunnels are generally conducted at relatively low Reynolds numbers, and even though many modern light aircraft are equipped with a canard wing operated in the low- Reynolds number range, Reynolds number effects on the vortex roll-up process are not well understood. It is the purpose of this work to contribute additional experimental results to the problem and compare these to existing models. With this objective, flow visualization techniques, both in air and in water, and laser Doppler velocimetry were used to examine the flow around a representative foil model.

Experiments

The foil chosen for this study had an elliptic planform with an aspect ratio of 3 and a NACA 66_2-415 ($a=0.8$) cross section. The angle of zero lift α_0 for this cross section is -2.5 deg. The half-span of the foil was 152.4 mm, and the mean chord c_m was 101.6 mm. Dye injection holes, each connected to an independent tube, were placed close to the leading edge on the pressure side for flow visualization in water.

Surface oilflow visualizations were conducted in air to study the behavior of the foil boundary layer. These visualizations were carried out in a low-speed open-return wind tunnel with a 43.2×30.5-cm test section and freestream velocities which could be varied from 18–70 m/s. Various Reynolds numbers were tested up to $Re_c=5.3\times10^5$ (based on the root chord, 129.4 mm). A mixture of a light mineral oil and titanium dioxide was used as a flow tracer. The visualizations were conducted at Reynolds numbers as low as 1.35×10^5, also using a smaller foil with an 81-mm base chord.

The experiments in water were carried out in a 30.5-cm-wide water channel at a lower Reynolds number of 4.7×10^4. The dye visualizations were conducted using multiple dye injection holes on the foil and observing the streakline development downstream. The measurements of the tip-vortex velocity profiles were carried out in the water channel with a Model 9100-2, TSI laser Doppler velocimeter (LDV). This system included a 5-mW Helium-Neon laser, a ($2.27\times$) beam expander, and a 120-mm focusing lens. The use of the beam expander was necessary to achieve adequate space resolution, reducing the calculated probe volume to 0.46 mm in length and 0.07 mm in width. The output of the TSI frequency tracker was analyzed on-line with an HP9836A microcomputer.

Axial (z direction) and tangential (x direction) velocity components were measured across the vortex. The traverses were carried out in planes perpendicular to the vortex axis at three axial locations ($z/c=0.785$, 1.57, and 3.93) along the y-axis direction normal to the wing span. Two methods were used to measure the tangential velocities. In the first, the tangential component was measured directly by aligning the probe-volume fringes with the freestream velocity direction, a procedure which is satisfactory if the tangential velocity is above a certain minimum (about 10 cm/s in the case of the present experiments). In the second, the beams were rotated to measure, at each point, first the axial velocity component and then a component at 45 deg to the freestream velocity. The tangential component was then calculated from these measurements. The latter procedure was necessary near the

Presented as Paper 86-0562 at the AIAA 24th Aerospace Sciences Meeting, Reno, NV, Jan. 6–9, 1986; received July 8, 1986; revision received April 21, 1987.

*Assistant Professor, Department of Aerospace Engineering and Mechanics. Member AIAA.

†Teaching Assistant, Department of Civil & Mineral Engineering, presently Consulting Engineer, Sao Paulo, Brazil.

‡Professor, St. Anthony Falls Hydraulic Laboratory, Department of Civil and Mineral Engineering.

vortex axis, since the tangential velocity is zero at the axis and the LDV used did not have, at the time, a Bragg cell for frequency shifting. Complete details of the experiment setup are given in Ref. 9.

Experimental Results

Flow Visualizations

Extensive oilflow visualizations on the foil surfaces were conducted in air at various angles of attack and Reynolds numbers. Figures 1a–1f and 2 show sample results from the oilflow visualizations. At small angles of attack, a separation bubble with its leading edge at 60–65% of the chord was visible over the suction side of the foil at Reynolds numbers between 2.7×10^5 and 5.3×10^5 (Figs. 1a and 1b). At the higher Reynolds number, reattachment occurs at approximately 75% of the chord, while at the lower Reynolds number, the last 35% of the chord is almost entirely separated. At even lower Reynolds numbers (1.35×10^5), the leading edge of the separation zone appeared at about the same location, but the flow did not reattach. These results agree fairly well with analytical predictions presented later.

Figures 1c and 1d depict the flow over the suction side of the foil at a higher angle of attack, for which analytical predictions of separations very likely require consideration of the large streamline curvature near the leading edge. Such predictions were not attempted in this work. The effect of the Reynolds number is clearly seen in the figures. Figure 1c shows a separation bubble extending from 65% of the chord, with a smaller bubble length than in Fig. 1a. Figure 1d shows, on the other hand, that at the higher Reynolds number and the same angle of attack $\alpha-\alpha_0=12.5$ deg, the entire flow remains attached due to transition to turbulence, the location of which cannot be determined from the photographs. (A slight flow retardation could be observed near the leading edge, but no leading edge separation was evident.) The same phenomena was seen at 2.7×10^5, but at a slightly higher angle of attack.

At still higher angles of attack, the adverse pressure gradient was too large for even the turbulent boundary layer to remain attached (Figs. 1e and 1f). A leading edge separation and a reattachment appeared at both Reynolds numbers, with a shorter separation zone at the higher Reynolds number, as expected. (The tunnel boundary layer was kept to a minimum, but a small interference was seen at the base chord near the trailing edge, which was subsequently reduced with an end plate.)

The pressure side of the foil also exhibited a separated zone and reattachment, as predicted, at the Reynolds numbers examined. The flow near the tip was directed toward it on the pressure side, an effect that was found to increase with increasing angle of attack. There was no leading edge separation. The typical flowfield at a high angle of attack is shown in Fig. 2.

When the boundary layer was tripped along the leading edge for comparison, the separated regions were eliminated on both pressure and suction sides except for cases where the natural transition occurred without trip. In these cases, the turbulent separation was observed in both tripped and clean foils.

The dye visualization experiments in water showed the roll-up phenomena clearly. At high angles of attack, the flow over the foil near the tip wrapped up much more quickly and the roll-up itself proceeded at a faster rate. For the angles of attack tested, the flow into the vortex core seemed to be coming from the region slightly away from the wing tip (see, e.g., Fig. 3). The flow farther away from the tip, on the other hand, appeared to proceed downstream without being entrained into the tip vortex. The flow separation over the foil, discussed earlier, was also visible in these visualization experiments. It is to be noted that the intermittent appearance of the dye issuing from the port nearest the tip (Fig. 3) is due to an inadvertent interaction between the dye flow and the port.

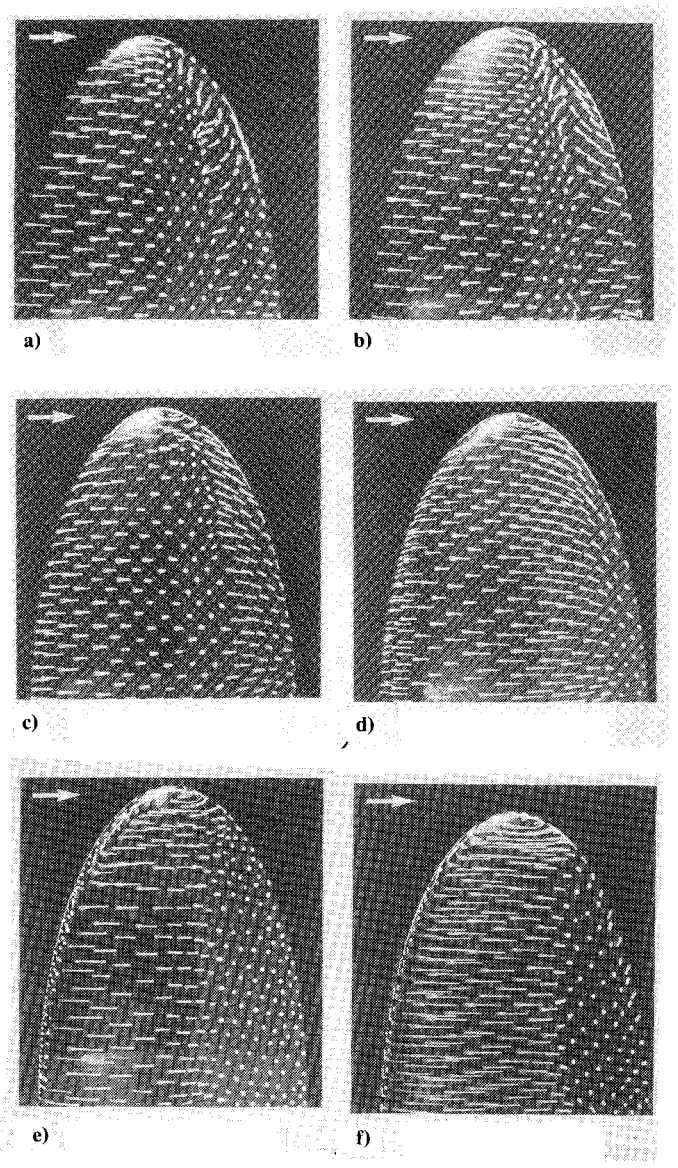

Fig. 1 Oil film visualizations on suction side: a) $\alpha-\alpha_0=7.5$ deg, $Re_c=2.7\times10^5$; b) $\alpha-\alpha_0=7.5$ deg, $Re_c=5.3\times10^5$; c) $\alpha-\alpha_0=12.5$ deg, $Re_c=2.7\times10^5$; d) $\alpha-\alpha_0=12.5$ deg, $Re_c=5.3\times10^5$; e) $\alpha-\alpha_0=17.5$ deg, $Re_c=2.7\times10^5$; f) $\alpha-\alpha_0=17.5$ deg, $Re_c=5.3\times10^5$.

Velocity Measurements

Comparison of the two methods used to obtain the tangential velocity distributions as described earlier showed good agreement in regions of overlap. In fact, since the two-velocity-component method yields larger scatter than the direct measurement method (as can be seen from an analysis of standard deviations), both procedures were used jointly in the traverses, the first within the vortex core, the latter outside of it. (At low angles of attack and/or small Reynolds numbers, the two-velocity-component method had to be used almost exclusively due to the low values of the resulting velocities.)

Some vortex wandering was observed in both the vertical and horizontal planes. However, it was not sufficiently strong to affect in any significant manner the repeatability of results or the velocity profile plots, and no corrections as in Baker et al.[10] were introduced. Velocity traverses were made in the y direction at different spanwise positions (x values) to verify the position of the vortex center, made visible in all cases by the naturally entrained air bubbles. These measurements disclosed a marked noncircularity of the vortex structure which did not change appreciably when the foil was placed at different distances from the side wall to check for possible side wall interference effects.

Figure 4 shows the tangential velocity profiles measured at a distance of two mean chord lengths downstream from the tip for three angles of attack $\alpha-\alpha_0$ equal to 7.5, 12.5, and 17.5 deg. The core radius and the circulation can be seen to increase with angle of attack. The maximum tangential velocity was in all cases larger on the suction side than on the pressure side by about 10%. The velocity profiles measured at the other axial locations are not shown for reasons of brevity.

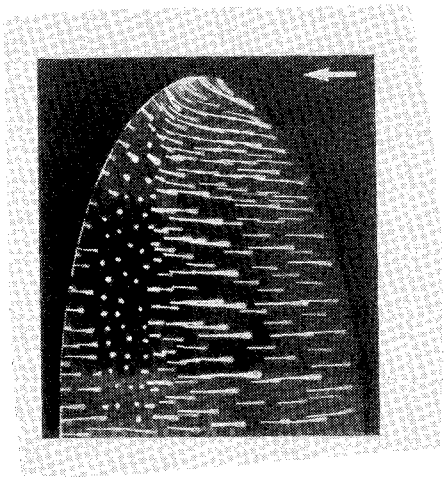

Fig. 2 Oil film visualizations on pressure side, $\alpha-\alpha_0=17.5$ deg, $Re_c=5.3\times10^5$.

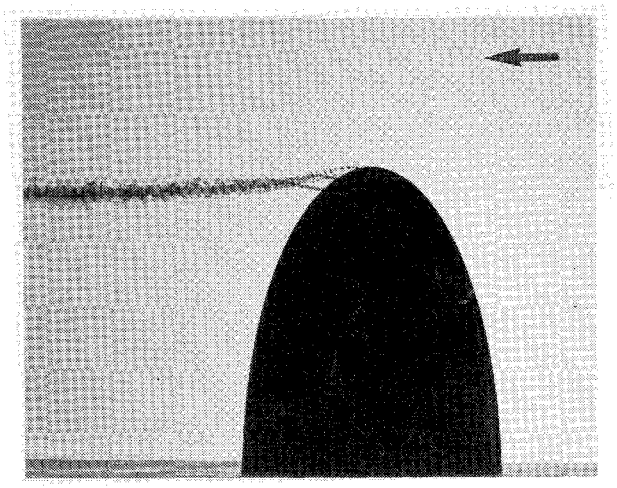

Fig. 3 Dye visualization of tip-vortex, $\alpha-\alpha_0=7.5$ deg, $Re_c=4.7\times10^4$.

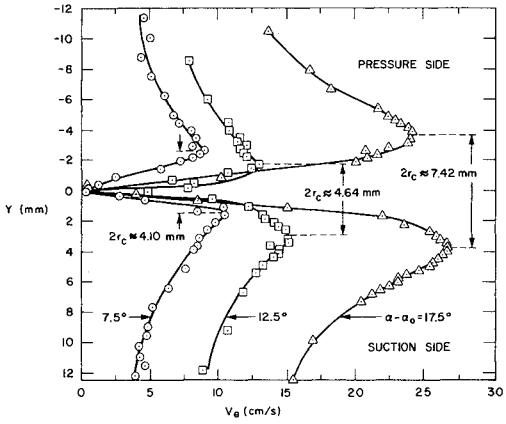

Fig. 4 Tangential velocity profiles at different angles of attack, $z/c_m=2$, $Re_c=4.7\times10^4$.

Discussion of Results

Flow Separation and Reattachment

As noted earlier, the flow visualizations clearly showed the flow separation from the foil at the relatively low Reynolds numbers of the experiments. Because of the possible effects of separation on the vortex roll-up process, this result was examined further. Starting with the two-dimensional inviscid pressure distribution along the foil, approximate calculations using the Karman-Pohlhausen method confirmed the occurrence of laminar separation at approximately 65% chord on both pressure and suction sides up to $\alpha-\alpha_0=7.5$ deg. At higher angles of attack, this method predicted laminar separation near the leading edge of the suction side. For these higher angles of attack, however, analytical predictions of separation very likely require consideration of the large streamline curvature near the leading edge, and the present predictions cannot be considered reliable. Thwaites' boundary-layer method was also applied to the present configuration to obtain estimates of boundary-layer thickness and other parameters.[11] The predicted separation locations, which are independent of the Reynolds number, were approximately the same as those predicted by the Karman-Pohlhausen method. Boundary-layer stability calculations showed laminar boundary-layer flow up to the separation point. With the computed boundary-layer parameters, Gaster's[12] results were used to determine whether the separation bubble was "long" or "short." Because the local chord Reynolds number decreases toward the tip, an inherent three-dimensional reattachment pattern was generated. The predicted flow pattern for a moderate angle of attack $\alpha-\alpha_0=7.5$ deg at $Re_c=5.3\times10^5$, corresponding to the experimental conditions of Fig. 1b is shown in Fig. 5. A short bubble was predicted to extend almost to the tip, and a long bubble was predicted in the tip region. The experimental results in Fig. 1b substantiate the prediction, and the spanwise pressure gradient due to the varying separation bubble length is seen generating the three-dimensional flowfield on the foil. The flow in the region near the tip ("long bubble") appears to be more complex than predicted by the present two-dimensional model. At a lower Reynolds number $Re_c=2.7\times10^5$, the calculations predicted a short bubble of larger length extending over about two thirds of the foil, the long bubble extending then over a larger area from the tip inward. The prediction was thus for the flow to reattach downstream up to a certain spanwise location from the base chord and to remain separated near the tip. Compared with the experimental results in Fig. 1a, the size of the separation bubble was underpredicted, but otherwise a good agreement was observed. At the low Reynolds number of the water-channel experiments, flow reattachment does not occur after the initial laminar separation.

The effects of the separation and reattachment on a two-dimensional wing section at low Reynolds numbers have been recently reviewed by Mueller.[13] In the present experiment, even though an elliptic planform was used, the actual load distribution may not have been elliptic. The positions of the separation and reattachment lines are of obvious importance in the determination of the circulation and lift of the airfoil. Besides altering the circulation distribution, flow separation could also significantly affect the flow pattern and the amount of fluid entrained by the vortex, and this indicates the desirability of further study of these three-dimensional aspects of the problem.

Flowfield

The oilflow visualizations on the suction side of the wing (see Fig. 1) showed some tipward fluid motion in the region near the wing tip, particularly at the larger angles of attack. Additionally, the dye visualizations in the water channel seemed to indicate, again at the larger angles of attack, entrainment of fluid from the suction side into the vortex core, though unfortunately the positions of the dye injection holes

on the wing did not allow for completely satisfactory pictorial evidence of this process. Qualitatively, these visualizations pointed to a role of the suction side of the wing in the initial stages of the vortex roll-up. This effect, which had already been noted by other researchers (Souders et al.,[14] Francis,[15] Billet[16]), casts doubts upon McCormick's[17] assumption that the pressure-side boundary layer is the essential factor in determining the size of the vortex core. Furthermore, McCormick's additional assumption that the vortex core is formed by fluid that leaves the foil from its tip appears questionable, as noted earlier. In general, the present flow visualizations seem to indicate a strong effect of angle of attack on the initial stages of the roll-up process.

Vortex Structure

The tangential velocity measurements clearly show the asymmetry of the vortex in the direction of the traverse. While one would not expect the tangential velocity to be symmetric, it is to be noted that the larger velocity maximum is observed on the suction side of the foil. The nonsymmetrical nature of the roll-up is also evident from the recent numerical simulations,[3,18,19] even though accurate three-dimensional velocity profiles do not appear to have yet been measured or calculated. In this respect, the present traverses on planes not containing the vortex axis disclosed larger vortex core radii (with smaller maximum tangential velocities), indicating that the vortices are indeed not circular in shape, but might possibly have a Cassini oval shape.

An axial velocity defect was present in the vortex core as expected but was much larger than that observed by Baker et al.,[10] for example, which could be due to the presence of a large separated region at the low Reynolds numbers of the LDV experiments. Though not shown for brevity, the profiles were Gaussian-shaped. The magnitude of the velocity defect was found to be as much as 40% of the freestream velocity at the larger angle of attack ($\alpha - \alpha_0 = 17.5$ deg) and decreased almost linearly with angle of attack.

Vortex Core Radius

Figure 6 shows the core radii measured at different axial positions plotted as functions of the viscous parameter $\sqrt{(\nu z/U_0)}$. The third set of points corresponds to the same location as the second set but with a lower freestream velocity. The vortex radii were obtained from the positions of the two tangential velocity maxima. Accurate determination of the locations of these maxima is difficult, as can be seen immediately from an examination of the velocity plots. Since in addition the core is inherently asymmetric, as discussed earlier, the error in core radius estimates may be considerable and could be as high as 20% in some cases. Bearing this in mind, the present results were compared with theoretical results obtained applying the theories of Prandtl,[5] Moore and Saffman,[6] and McCormick.[17] Betz's model[4] is naturally not applicable, having a singularity near the origin. Prandtl's theory, which uses the Rankine velocity profile, gives values which are an order of magnitude larger than those presently observed. Moore and Saffman's model predicts reasonably well the variation of the radius with downstream distance, as shown in Fig. 6, but fails to predict the influence of the angle of attack, which was found essential to the determination of the core size. The same is true of the growth rates predicted on the basis of Lamb's line vortex model or Squire's constant eddy viscosity model, both of which produce the same functional relationship for vortex core growth as does Moore and Saffman's. The core radius was found to increase with decreasing Reynolds number, as comparison of the second and third sets of points in Fig. 6 indicates.

McCormick's semiempirical core radius equation was found to provide a good estimate of the core size in the range of Reynolds numbers studied (see Ref. 9), although it does not take downstream distance into account or represent physical phenomena observed in the present flow visualizations. The underlying assumptions of this model, however, require further experimental study.

Tangential Velocity Distribution

The tangential velocity profile is linear within the vortex core and exhibits some rounding off as the peak velocities are approached from inside the core. Outside the vortex core, the velocity distribution obeys an r^n power law, with the exponent n varying with outward distance from the vortex centerline. In the present experiments, a large amount of circulation was found still to exist outside the vortex core at all downstream distances, likely due to a thick vorticity-containing shear layer as will be discussed later. A value of $n \approx -0.6$ was obtained in the region where the roll-up is proceeding. Coincidentally, this is not too far from the theoretical value of -0.5 that can be predicted for an elliptically-loaded wing using Betz[4] inviscid analysis, which does not include a prediction of vortex core flow. Normalized velocity profiles based on other models are shown in Fig. 7, together with the present experimental results. All of the models are axisymmetric and, since the figure is normalized, we also note that the magnitude of the maximum tangential velocity varies considerably among models. Maximum velocities calculated using Moore and Saffman's model,[6] for example, produced velocities on the average 30% above the measured values. The Rankine model assumes a solid-body rotation within a core and a potential flow outside. The Lamb model also has the vorticity almost entirely enclosed within a core. Both models present too rapid a velocity decay outside the core. Squire's turbulent model[20] gives the same normalized profile as the Lamb model except for a faster growth of the vortex core corresponding to a higher value for his constant eddy viscosity. Staufenbiel's recent analysis[8] presents a

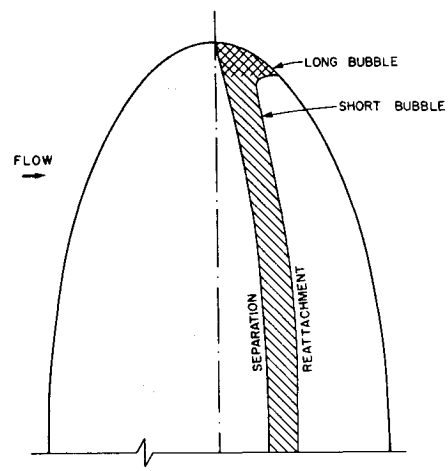

Fig. 5 Prediction of boundary-layer separation, $\alpha - \alpha_0 = 7.5$ deg, $Re_c = 5.3 \times 10^5$ (this corresponds with Fig. 1b).

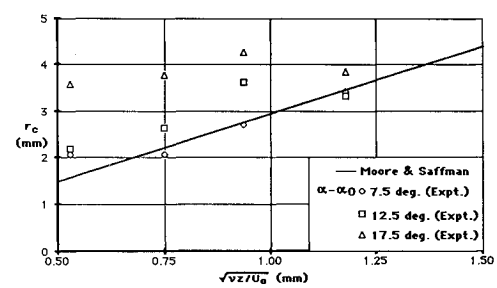

Fig. 6 Variation of vortex core radius with downstream distance at different angles of attack (uncertainty of data ±20%).

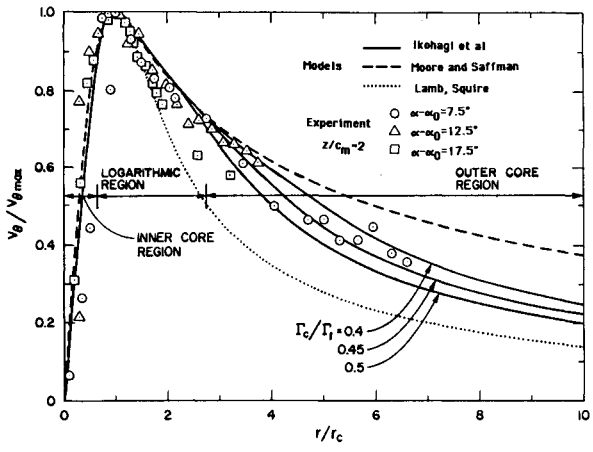

Fig. 7 Comparison of normalized tangential velocity profiles.

modified Lamb model which satisfies both the conservation of energy and the dispersion relationship. Once the velocity profile is normalized by a maximum tangential velocity and the core radius, however, the profile remains similar to Lamb's model, even though the circulation within the core was an adjustable parameter of the model.

It should be noted that the core circulation Γ_c has been measured by various investigators to be a small fraction of the total vortex circulation Γ_1 at a given axial distance (see, e.g., Govindaraju et al.[21]). The core circulations Γ_c measured in the present experiments varied between 13 and 24% of the theoretical midspan circulation Γ_0 and were considerably lower than values reported earlier. The velocity profiles measured at all downstream stations showed clearly that a large fraction of the vortex circulation remained outside the core. Although the data did not extend far enough radially to determine the total circulation unambiguously, the total vortex circulation Γ_1 was found to grow gradually downstream at a rate consistent with Kaden's analysis[22] and the calculations by Moore[18] and Bilanin et al.[23] (A more detailed comparison of the present data and these calculations is presented in Ref. 24.) The magnitude of the vortex circulation, however, increased to only approximately 45% of Γ_0, even at a downstream distance of four mean chord lengths. This low value is undoubtedly due in part to a reduction in circulation around the separated foil, in part to vorticity dissipation and diffusion in the wake of the wing. With boundary-layer separation around the foil, a thicker viscous region should result downstream from it, and this can produce both larger dissipation and vorticity diffusion rates, the latter leading to a larger fraction of circulation outside the core upon roll-up. No lift measurements and flow visualizations at lower Reynolds numbers were undertaken that would permit a quantitative discussion of this point.

An empirical vortex model recently proposed by Ikohagi et al.[24] consists of a core region, a logarithmic region similar to the turbulent vortex model of Hoffman and Joubert,[25] and an outer core region. In this model, the circulation contained in the vortex at a given distance from the trailing edge is allowed to grow as experimentally observed in a manner similar to Moore's[18] and Bilanin et al.'s[23] numerical results, which is also consistent with Kaden's[22] analysis. With the ratio of core circulation to vortex circulation as a parameter to be fitted, the velocity profiles compare well with the present measurements, as seen in Fig. 7.

Conclusions

At the moderately low Reynolds numbers tested, strong viscous effects were observed throughout the flowfield from the boundary layer on the foil to the vortex roll-up region. Laminar, and in some cases turbulent, boundary-layer separations were observed on the pressure and suction sides of the foil throughout the entire range of Reynolds numbers covered in this study. The locations of laminar separation agreed well with predictions based on laminar boundary-layer calculations. Laminar separation with long and short bubbles was observed in a manner consistent with the predictions. Since the local chord Reynolds number varies across the span, different separation bubble lengths resulted. This causes three-dimensional flow patterns due to strong spanwise pressure gradients.

The vortex circulation was found to increase gradually with downstream distance. Even though the rate at which the circulation increased was consistent with previous analyses and numerical results, the magnitude of the total circulation was estimated to be at most 45% of the theoretical midspan circulation, even at a downstream distance of four mean chord lengths. This was in part caused by a reduced circulation around the separated foil but also by dissipation of vorticity in the wake.

The core circulation contained a very small fraction of the theoretical midspan circulation. A large fraction of the circulation remained outside the core, resulting in a more gradual velocity decay with radius than that given by Rankine or Lamb models. The tangential velocity distribution is roughly linear inside the vortex core. Outside the core, the velocity does not obey a $1/r$ power law like a potential flow but decays rather slowly, indicating a large amount of vorticity diffusion. The exponent of r was seen to vary depending upon several factors and appeared to change with outward distance. A recently developed empirical vortex model allowed for reasonably good agreement with the experimental results, but more work is needed for elucidation of the mechanics of the roll-up.

The flow into the core of the tip-vortex is most probably affected by the boundary layers on both the suction and pressure sides of the wing, to a greater or lesser extent depending upon the angle of attack. It does not necessarily originate at the tip of the foil, but proceeded at times from inboard positions on the trailing edge. Flow visualization on the pressure side of the foil showed a strong outward flow near the tip at high angles of attack, indicating that more fluid is swept into the core as the angle of attack increases.

The radius of the tip-vortex core was seen to increase with angle of attack and downstream distance and decrease with Reynolds number. McCormick's semiempirical equation for the core radius provided an adequate estimate of the core size in the range of Reynolds numbers studied, although it does not take downstream distance into account. Moore and Saffman's model, on the other hand, predicts reasonably well the variation of the radius with distance but fails to predict the influence of angle of attack, which is fundamental to the determination of the core size.

Acknowledgments

This work was supported in part by the Office of Naval Research. Under the direction of the first author, Mr. A. McGettrick participated in the oilflow visualization studies, with support from the Undergraduate Research Opportunities Program of the University of Minnesota.

References

[1]Donaldson, C. duP. and Bilanin, A. J., "Vortex Wakes of Conventional Aircraft," AGARD-AG-204, May 1975.

[2]Platzer, G. P. and Souders, W. G., "Tip Vortex Cavitation Delay with Application to Marine Lifting Surfaces, A Literature Survey," Research and Development Rept., David Taylor Naval Ship Research and Development Center, DTNSRDC-79/051, Aug. 1979.

[3]Hoeijmakers, H. W. M., "Computational Vortex Flow Aerodynamics," *Aerodynamics of Vortical Type Flows in Three Dimensions*, AGARD Conference Proceedings No. 342, 1983, pp. 18.1-18.35.

[4]Betz, A., "Behavior of Vortex Systems," NACA TM-713, June 1933 (translated from ZAMM, Bd. XII, No. 3, June 1932).
[5]Durand, W. F., "Aerodynamic Theory," Vol. II, Div. E, Julius Springer, 1935.
[6]Moore, D. W. and Saffman, P. G., "Axial Flow in Laminar Trailing Vortices," *Proceedings of the Royal Society of London*, A333, 1973, pp. 491-508.
[7]Phillips, W. R. C., "The Turbulent Trailing Vortex during Roll-Up," *Journal of Fluid Mechanics*, Vol. 105, 1981, pp. 451-467.
[8]Staufenbiel, R. W., "Structure of Lift-Generated Rolled-Up Vortices," *Journal of Aircraft*, Vol. 21, Oct. 1984, pp. 737-744.
[9]Quadrelli, J. C., "An Experimental Investigation of Vortex Roll-Up for an Elliptically-Loaded Wing," M. S. Thesis, Univ. of Minnesota, Minneapolis, MN, 1985.
[10]Baker, G. R., Barker, S. J., Bofah, K. K., and Saffman, P. G., "Laser Anemometer Measurements of Trailing Vortices in Water," *Journal of Fluid Mechanics*, Vol. 65, Pt. 2, Aug. 1974, pp. 325-336.
[11]Arakeri, V. H., private communications, 1985.
[12]Gaster, M., "The Structure and Behavior of Laminar Separation Bubbles," NPL Aero Rept. 1181 (Revised), March 1967.
[13]Mueller, T. J., "Low Reynolds Number Vehicles," AGARDograph 288, 1985.
[14]Souders, W. G. and Platzer, G. P., "Tip Vortex Cavitation Characteristics and Delay of Inception on a Three-Dimensional Hydrofoil," Research and Development Rept., David Taylor Naval Ship Research and Development Center, DTNSRDC-81/007, April 1981.
[15]Francis, M. S., "A Wind Tunnel Investigation of the Formation of Trailing Vortices," Ph.D. Thesis, Univ. of Colorado at Boulder, CO, 1976.
[16]Billet M. L., private communications, 1984.
[17]McCormick, B. W. Jr., "On Cavitation Produced by a Vortex Trailing From a Lifting Surface," *Journal of Basic Engineering*, Transaction of ASME, Sept. 1962, pp. 369-379.
[18]Moore, D. W., "A Numerical Study of the Roll-Up of a Finite Vortex Sheet," *Journal of Fluid Mechanics*, Vol. 63, 1974, pp. 225-235.
[19]Srinivasan, G. R., McCroskey, W. J., Baeder, J. D., and Edwards, T. A., "Numerical Simulation of Tip Vortices of Wings in Subsonic and Transonic Flows," AIAA Paper 86-1095, May 1986.
[20]Squire, H. B., "The Growth of a Vortex in Turbulent Flow," *The Aeronautical Quarterly*, Aug. 1965, pp. 302-306.
[21]Govindaraju, S. P. and Saffman, P. G., "Flow in a Turbulent Trailing Vortex," *The Physics of Fluids*, Vol. 14, No. 10, Oct. 1971, pp. 2074-2080.
[22]Kaden, H., "Aufwicklung einer unstabilen Unstetigkeitsfläche," *Ingenieur-Archiv*, Vol. 1, 1931, pp. 140-168.
[23]Bilanin, A. J. and Donaldson, C. duP., "Estimation of Velocities and Roll-Up in Aircraft Vortex Wakes," *Journal of Aircraft*, Vol. 12, No. 7, July 1975, pp. 578-585.
[24]Ikohagi, T., Higuchi, H., and Arndt, R. E. A., "The Structure of Trailing Vortices," *Advancement in Aerodynamics, Fluid Mechanics and Hydraulics*, ASCE Symposium, Minneapolis, MN, June 1986.
[25]Hoffman, E. R. and Joubert, P. N., "Turbulent Line Vortices," *Journal of Fluid Mechanics*, Vol. 16, Pt. 3, July 1963, pp. 395-411.